ICSV13 - Vienna
The Thirteenth International Congress on Sound and Vibration
Vienna, Austria, July 2-6, 2006

APPLICATION OF FEEDFORWARD STRUCTURES FOR ISOLATION OF CAR ENGINE VIBRATION

Jörg Paschedag* and Johannes L. R. Schwarz

Institute of Automatic Control (Prof. Dr.-Ing. habil. B. Lohmann),
Technical University Munich
Boltzmannstr. 15, Germany - 85748 Garching / Munich
paschedag@tum.de

Abstract

This paper reports about practical experience and algorithmic improvements in active isolation of engine induced vibration. The analysed control algorithms are implemented on an experimental setup that resembles the automobile structure of interest. All considered algorithms are of feedforward structure. An important condition of the given application is the availability of a tachometer signal. It provides improvement opportunities for the algorithms, which are discussed. The considered algorithms are compared with respect to performance and computational costs.

1. INTRODUCTION

In the automobile industry, significant effort is made to keep disturbing vibration away from the vehicles chassis. The aim is to improve ride comfort as well as preventing the mechanical structure from permanent exposure to oscillating forces. One important application of vibration control in the automobile is the isolation of engine induced vibration. This paper concentrates on the realization of suitable damping systems by active means, particularly by application of feedforward algorithms [3], [8].

After a more detailed description of the considered application and some fundamental information about the applied feedforward structure in Section 2, the third section concentrates on implementation issues of the well known filtered-x least mean squares algorithm (FxLMS). In the fourth section, other LMS-based algorithms are presented that, unlike the FxLMS, make use of recursive adaptive filters. In Section 5, two alternative feedforward approaches are considered that work exclusively for periodic excitation. The work concludes with a comparison of the applied algorithms regarding computational costs.

2. EXPERIMENTAL SETUP AND FEEDFORWARD PRINCIPLE

In an automobile, the engine generates vibration that is transmitted via the engine mounts to the cars chassis. The experimental setup shown in Figure 1 has been constructed to analyse this transmission of vibration. Basic element of the setup is an industry-manufactured chassis subframe on which the engine is mounted in the real car. The subframe itself is mounted at four points to a bedplate that stands for the cars chassis. Two force actuators (reaction mass type) are installed on the subframe. *Actuator 1* represents the engine and induces the unwanted vibration which is composed of sinusoidal signals of a basic frequency F_b and its harmonics. *Actuator 2* is used for vibration cancellation at one mounting point of the subframe.

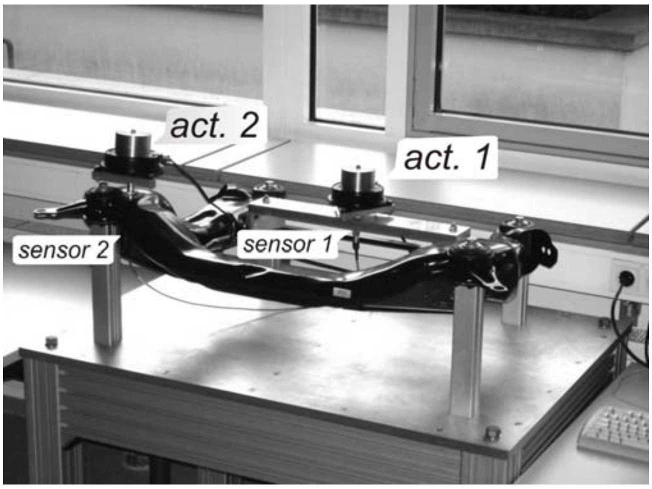

Figure 1 – experimental setup with chassis subframe

For vibration measurement, two accelerometers are positioned directly at the mounting locations of the actuators. Anti-aliasing and signal reconstruction is accomplished by analog butterworth filters of order eight with 300*Hz* cut-off frequency.

The block diagram in Figure 2 illustrates the principle of the feedforward structure applied to the given application.

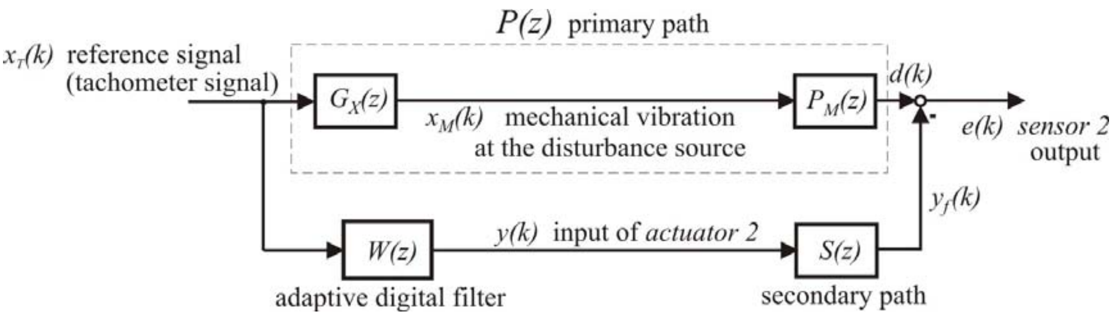

Figure 2 – applied feedforward structure

The reference signal $x_T(k)$ is related to the source of the disturbing vibration. It is fed forward in the signal flow in order to achieve disturbance cancellation by superimposing the “anti-signal” $y_f(k)$ to the signal $d(k)$. Commonly, the reference signal is chosen to be a sensor signal (here of *sensor 1*). However, for the given application, the sensor measurement can be replaced by a tachometer signal. Idealised, the tachometer signal is an impulse train with a frequency equal to the basic frequency F_b of the engine vibration. In many cases, such a signal can be received directly from the cars electronic system. The use of the tachometer signal makes *sensor 1* dispensable. Moreover, disturbing feedback effects of the cancelling *actuator 2* on the reference *sensor 1*, which affect the stability of the adaptive algorithm, are avoided [3]. The tachometer signal is suitable as reference signal because the spectrum of an impulse train with frequency F_b includes exactly the frequency components of the engine vibration: The basic frequency F_b and its harmonics. The adjustment of magnitude and phase can be considered to be performed by the transfer function $G_x(z)$. The output of $G_x(z)$ is the mechanical engine vibration $x_M(k)$ which is transmitted to the cancellation point by the path $P_M(z)$. Perfect cancellation is achieved, if the adaptive digital filter $W(z)$ is parameterised such that $W(z)=P(z)S(z)^{-1}$.

Note that the original tachometer signal has to be filtered by an analog anti-aliasing filter before it is A/D-converted for digital signal processing. Otherwise, the frequency components will be corrupted if the current sampling frequency F_S is not an integer multiple of the basic frequency F_b.

The periodicity of the engine induced vibration is a necessary condition for the realizability of feedforward systems for the given application. It provides that no causality constraint has to be met [3] since the signal processing of the adaptive algorithms can refer to the signals delayed for an (theoretically) arbitrary number of periods whenever necessary.

3. IMPLEMENTATION OF THE FXLMS-ALGORITHM

A most commonly used adaptive algorithm for the realization of feedforward AVC-systems is the FxLMS algorithm [1], [2]. Its basic structure is depicted in Figure 3 in a similar notation as used by Kuo and Morgan in [3].

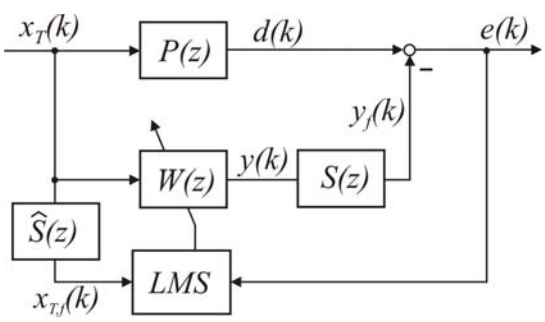

Figure 3 – FxLMS algorithm

A least mean squares (LMS) algorithm is employed to update the coefficients of $W(z)$ in such a way that the expected value of the squared error signal $e^2(k)$ converges to zero over time. The filter $W(z)$ is realized as a finite impulse response (FIR) filter. Since all poles of such a filter are fixed at zero, it is inevitably stable. The applied recursive formula for the update of the filter coefficients $\boldsymbol{w}(k)=[w_1(k), w_2(k),\ldots,w_n(k)]^T$ *is*

$$\boldsymbol{w}(k+1) = \beta\,\boldsymbol{w}(k) + \frac{\alpha}{P_{xTf}(k)\cdot n}\,\boldsymbol{x}_{T,f}(k)e(k) \quad , \tag{1}$$

again in a similar form as stated in [3]. In (1), $\boldsymbol{x}_{T,f}(n)$ is a vector containing the last n samples of the signal $x_{T,f}(k)$ in reversed order of their occurrence: $\boldsymbol{x}_{T,f}(k) = [x_{T,f}(k),\ x_{T,f}(k\text{-}1)\ ,\ \ldots\ ,\ x_{T,f}(k\text{-}n)]^T$. The parameter β is the so called leakage factor. It prevents the coefficients of the Filter W from diverging when the spectral excitation of the algorithm is not sufficient. The quotient $\alpha/(P_{xTf}(\mathrm{k})\cdot n)$ in (1) provides a normalized step size that takes into account the dependence of the algorithms stability on the power $P_{xTf}(k)$ of the signal $x_{T,f}(k)$. An estimation of $P_{xTf}(k)$ can be calculated by $P_{xTf}(k)=[\boldsymbol{x}_{T,f}(k)^T\cdot\boldsymbol{x}_{T,f}(k)]/n$. For a successful practical application, it is important to limit the value of $P_{xTf}(k)$ to a certain minimum $P_{xTf,min}$. Thus, the step size μ will not tend to infinity if the actual power of the excitation signal gets close to zero. The digital filter $\hat{S}(z)$ in Figure 3 is a model of the secondary path $S(z)$. It has been implemented as an FIR filter of length n_{sec}=200.

Since the engine vibration is periodic, the order n of the filter W can be chosen such that its finite impulse response is longer or equal to one period of the lowest possible basic frequency $F_{b,min}$ of the engine vibration: $n \geq F_S / F_{b,min}$. Suitable values for the other critical parameters are presented in the next section, together with the achieved damping results.

4. APPLICATION OF RECURSIVE ADAPTIVE FILTERS

Infinite impulse response (IIR) filters potentially need fewer coefficients than FIR filters to approximate a given system due to their recursive structure. Therefore, they are in general interesting for adaptive identification applications because a reduction of computational costs could be expected. On the other hand, adaptive IIR filters can become unstable. Moreover, their performance surface is generally nonquadratic and multiple local minima are possible [4].

Effective algorithms for adaptation of recursive filters have been developed on basis of the LMS algorithm. A cost-efficient one, the recursive LMS algorithm, has been proposed in [5]. Based on this is the filtered-u LMS (FuLMS) algorithm, proposed in [6]. The FuLMS algorithm takes in account the presence of the secondary path *S(z)* and can be applied to AVC-systems like the one considered here. In Figure 4, the structure of the FuLMS is shown with an additional modification: An FIR filter *C(z)* is applied to the error signal before it is fed to the LMS-algorithms. The aim of this is a smoothing of the error signal and therefore an increased stability margin of the adaptation process. The resulting algorithm is called SHARF (simple hyperstable adaptive recursive filter) [7]. The coefficients of the filter $C(z)$ are commonly chosen to be the negated coefficients of the recursive part $B(z)$ of the IIR-filter [8]. The stability behaviour of the SHARF algorithm implemented in this way was mostly a little better and never worse than that of the original FuLMS. The recursive filter in Figure 4 is realized by two FIR filters $A(z)$ and $B(z)$ which are separately adapted by two FxLMS-algorithms as described in the previous section. Its mathematical description is

$$y(k) = \sum_{i=1}^{n_a} a_i x_T(n-i) + \sum_{i=1}^{n_b} b_i y(n-i) \quad . \tag{2}$$

An interesting result of the practical analysis of the adaptive IIR-filters is, that they can be implemented quite stable. Necessary condition for this is of course an appropriate setting of the critical parameters of the algorithm. A useful method to protect the system from effects of still possible instability is to automatically restart the adaptation process whenever the absolute value of a low pass filtered version of the input signal $y(k)$ (*actuator 2*) exceeds a certain limit.

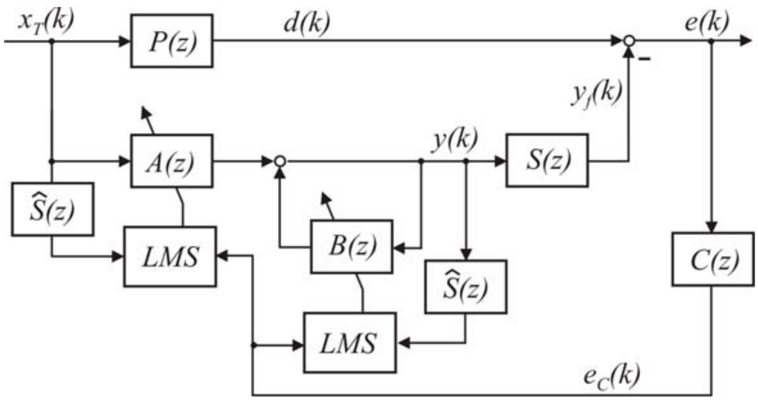

Figure 4 – FuLMS algorithm, extended to SHARF

The cancelling results of FxLMS and SHARF algorithm are compared with respect to the number of coefficients in Figure 5. Charted is the steady state RMS value of the error signal $e(k)$. The sampling frequency is F_S = 1000*Hz*. As excitation signal for *actuator 1*, a sum of sinusoids with a basic frequency of 25*Hz* and its harmonics up to 300*Hz* is applied. The parameters α_a and α_b denote the step sizes and β_a and β_b the leakage factors of the LMS-algorithms for the adaptation of the filters $A(z)$ an $B(z)$. The numbers of coefficients n_a and n_b are chosen in the way that $n_a=n_b+1$. It should be noted, that the results obtained from the FuLMs algorithm are quite similar to that of the SHARF.

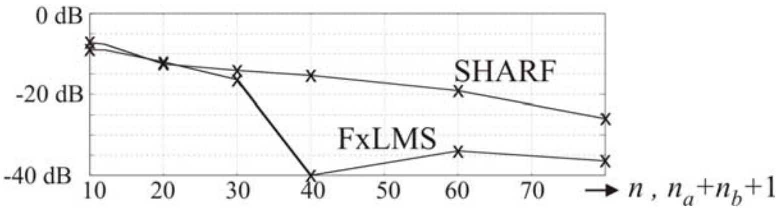

FxLMS:		SHARF:				for both:
α=0.05	β=0,99999	α_a =0.01	β_a =0.99999	α_b =0.005	β_b =0.99999	$P_{xTf,min}=10^{-6}$

Figure 5 – Steady state damping results and settings of FxLMS and SHARF

Figure 5 shows, that for the same overall number of filter coefficients the damping of the FxLMS algorithm is all in all far more effective than that of the SHARF method. Only at $n=n_a+n_b+1=20$, the SHARF algorithm performs insignificantly better. The same measurements have been performed at higher sampling rates F_S, but even then just a slight improvement of the SHARF algorithm compared to the FxLMS has been observed.

5. ALTERNATIVE ALGORITHMS

Two methods which depend crucially on the availability of a tachometer signal have been taken into account. The first of them is a so called waveform synthesis [9], [3], [8], as depicted in Figure 6. The shown structure is of extremely low computational costs and therefore seemed to be quite attractive. However, it was not possible to successfully implement it for the given application. The reason for this was, that the effect of the secondary path $S(z)$ can only be compensated for by approximating it by a delay time. This is due to the applied structure shown in Figure 6.

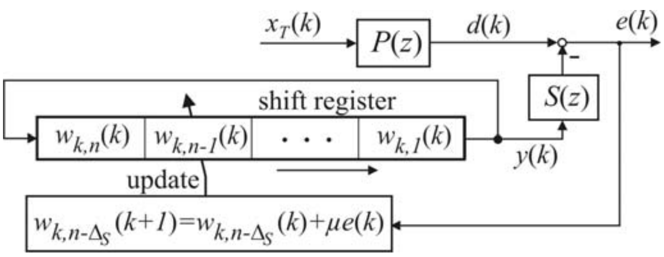

$w_{k,i}(k) = w_{((k+i-1) \bmod n)+1}(k)$

$n = round(F_S/F_b)$

$\Delta_S \cdot T_S$: Approximation of the secondary path by a delay time (here $\Delta_S=1$). It is $T_s=1/F_s$

Figure 6 – Algorithm for Waveform synthesis

In simulation, very promising results have been obtained as long as simple, fictitious secondary paths were used. For realistic secondary paths a stable behaviour of the algorithm could not be achieved.

The second considered approach depending on the existence of a tachometer signal was the application of single-frequency adaptive notch filters [10] in a parallel structure [3] as depicted in Figure 7.

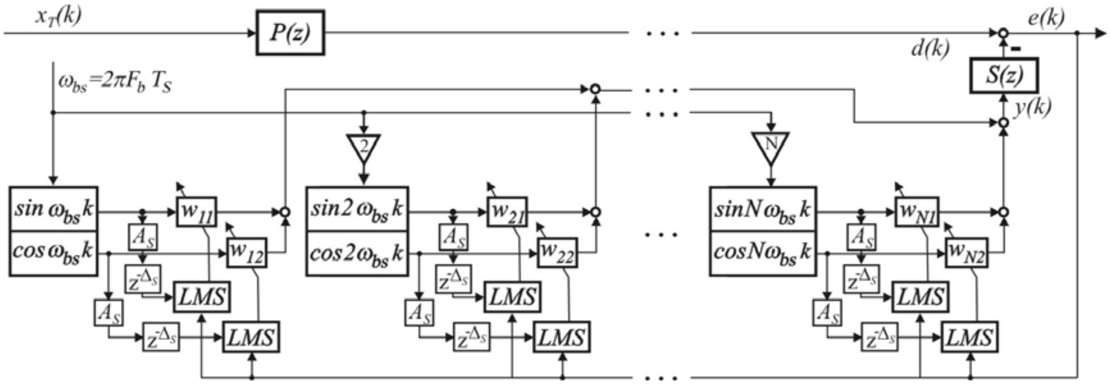

Figure 7 – parallel structure of adaptive notch filters

The adaptive notch filters do not require the impulse train tachometer signal directly as reference signal. Sine and cosine signals of the basic frequency F_b and its harmonics are used instead. Therefore only information about the frequencies of the signal components is needed. For the algorithm to work properly, this information must be very precise. It can be either received by measuring the time period of the impulse train tachometer signal by a high resolution timer or, if available, directly as a rotation rate signal from the cars electronic system.

Within the adaptation process, the sine and cosine inputs are tuned in amplitude. Thus, their superposition can provide harmonic signals of the amplitude and phase necessary to cancel the harmonic components in the disturbance signal d. The tuning of the amplitudes is performed by adaptive FIR filters with just one weight. With the structure in Figure 7, N harmonic signal components can be cancelled. To keep computational effort low, the secondary path models, which are necessary for a stable operation of the LMS-algorithms, have been simplified to a gain A_S and a delay time $\Delta_S \cdot T_s$. Both values are frequency dependent and were gained from amplitude and phase of the frequency response of the secondary path. They were implemented as vectors of the lengths $n_{S,Ampl}$=280 and $n_{S,Phase}$=280 .

With the adaptive notch structure of Figure 7, a robust and effective vibration cancellation was accomplished. Especially the achieved convergence speed was remarkably high. In Figure 8 it is compared to the other successfully implemented algorithms. The sampling frequency was again F_S = 1000Hz.

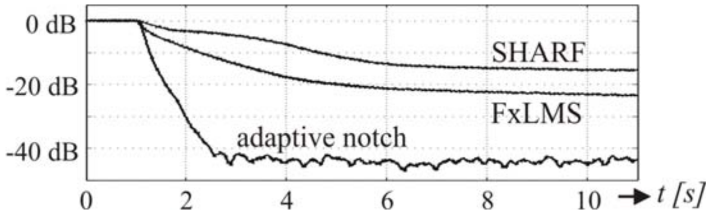

FxLMS and SHARF:	parallel adaptive notch structure			
same settings as in figure 6 and n= 50, n_a=25, n_b=24	α=0.005	β=1	$P_{xTf,min}$ =0.01	*for all LMS-blocks*

Figure 8 – convergence of the different algorithms

6. CONCLUSION

Three of the four considered feedforward algorithms have been applied successfully at the experimental setup. Of these, especially the parallel adaptive notch structure provided impressively good results regarding stability, degree of suppression and convergence speed. The comparison in table 1 indicates, that this approach might

Table 1 – Comparison of computational costs

Algoithms	Memory space	Multiplications	Summations	Extra
FxLMS (leaky+normalized)	$4n+2n_{sec}+3$	$4n+n_{sec}+1$	$3n+n_{sec}-3$	
FuLMS (leaky+normalized)	$4n_a+4n_b+4n_{sec}+6$	$4n_a+4n_b+2n_{sec}+2$	$3n_a+3n_b+2n_{sec}-5$	
SHARF (add. to FuLMS)	n_b	n_b	n_b-1	
Parallel adaptive notch (normalized)	$6N+n_{S,Ampl}+n_{S,Phase}$	$7N$	$3N-1$	sine generator / lookup table

also be the best choice regarding computational cost. Necessary condition for this is however a cost effective realization of the included sine generators as well as a memory saving implementation of the frequency dependent values A_S and Δ_S for the secondary path approximation. These implementation issues as well as a search for possibly better algorithmic configurations, like employment of the adaptive notch filters in cascaded form [11] will be concern of future work.

REFERENCES

[1] B. Widrow and M.E. Hoff, “Adaptive switching circuits”, *1960 IRE WESCON Convention Record*, New York IRE, pp. 96-104, 1960.

[2] D.R. Morgan. “An Analysis of Multiple Correlation Cancellation loops with a Filter in the auxiliary Path”, IEEE Trans. on Acoustics, Speech and Signal Processing, ASSP- **28**, 454-467, August 1980.

[3] S.M. Kuo, D.R. Morgan, “Active Noise Control Systems”, John Wiley & Sons, New York 1996.

[4] B. Widrow, S.D. Stearns, “Adaptive Signal Processing”, Prentice Hall, Upper Saddle River, New Jersey 1985.

[5] P. L. Feintuch. “An Adaptive Recursive LMS Filter”. Proc. IEEE, **64**, pages 1622-4, Nov 1976.

[6] L. J. Eriksson, “Active Sound Attenuation Using Adaptive Digital Signal Processing Techniques,” PhD. dissertation, Univ. Wisconsin, Madison, Wisconsin, Aug. 1985.

[7] M. G. Larimore, J.R. Treichler, and Jr. C.R.Johnson. “SHARF: An algorithm for adapting IIR digital filters”, IEEE Trans. on Acoustics, Speech and Signal Processing, **28**, 428–440, August 1980.

[8] C.H. Hansen, S.D. Snyder, Active Control of Noise and Vibration, E & FN Spon, London, 1997

[9] G. B. B. Chaplin: ”Anti-sound - The Essex breakthrough“, Chartered Mechanical Engineer (CME) **30**, 41–47, Jan. 1983.

[10] B. Widrow, J. R. Glover, J. M. McCool, J. Kaunitz, C. S. Williams, R. H. Hearn, J. R. Zeidler, E. Dong Jr., and R. C. Goodlin, “Adaptive noise canceling: Principles and applications,” Proc. IEEE, **63**, 1692-1716, 1975.

[11] D. R. Morgan and J. Thi, “A multitone pseudocascade, filtered-X LMS adaptive notch filter”, IEEE Trans. Signal Processing, **41**, 946-956, Feb 1991.